Chinese Chemical Letters 32 (2021) 3548–3552

Contents lists available at ScienceDirect

Chinese Chemical Letters

journal homepage: www.elsevier.com/locate/cclet

Communication

High temperature thermo-photocatalysis driven carbon removal in direct biogas fueled solid oxide fuel cells

Doudou Gu[a,c], Guan Zhang[a,c,*], Jing Zou[b,**]

[a] Institute of Hydrogen and Fuel Cell, Harbin Institute of Technology, Shenzhen, Shenzhen 518055, China
[b] General Education Division, School of Humanities & Social Science, The Chinese University of Hong Kong, Shenzhen, Shenzhen 518172, China
[c] School of Civil and Environmental Engineering, Harbin Institute of Technology, Shenzhen, Shenzhen 518055, China

ARTICLE INFO

Article history:
Received 17 January 2021
Received in revised form 26 January 2021
Accepted 28 January 2021
Available online 2 February 2021

Keywords:
Thermo-photocatalysis
Infrared light excitation
Carbon removal
Biogas utilization
Solid oxide fuel cells

ABSTRACT

Solid oxide fuel cells (SOFCs) can directly convert renewable biogas into electricity with high efficiency at high temperature, however the long-term stability of SOFCs is significantly affected by the carbon deposition on the anode during cell operation. Herein, we report a novel carbon removal approach by high temperature infrared light driven photocatalytic oxidation. Upon the comparison of electrochemical performance of Ni-YSZ anode and TiO_2 modified Ni-YSZ anode in the state-of-the-art single cell (Ni-YSZ/YSZ/LSCM), the modified anodes exhibit markedly improved peak powder density with simulated biogas fuel (70% CH_4+ 30% CO_2) at 850 °C with less coking after 40 h operation. The high activity and carbon deposition resistance of the modified anode is possibly attributed to the *in situ* generated hydroxyl radical from the reduced TiO_x powder under high temperature infrared light excitation, which is supported by detailed analysis of microstructural information of anodes and the powder-based thermo-photocatalytic experiments.

Abundant biogas produced from anaerobic treatment process of municipal wastewater and digestion of solid organic wastes can be employed as a renewable energy source. Conventional direct combustion of biogas produces thermoelectricity, but suffers from low efficiencies and emission of a variety of green-house gas pollutants such as NO_x, SO_x, CH_4 and CO_x into the air [1]. Solid oxide fuel cells (SOFCs) provide an alternative solution of direct employment with the biogas fuel and efficiently generate electricity using low-cost electrocatalysts [2]. Recently, there is increasing research on this type of directly biogas fueled SOFCs from single cells to complete stacks [3]. However, one of the significant issues limiting the further development of biogas fueled SOFCs is the carbon deposition on the anode, which results in the rapid performance degradation of the SOFCs cells [4]. Therefore, extensive work has been focused on the development of SOFCs cells with coking-resistant capability [5]. There are several strategies addressing this problem, one of which is adding the oxygen content in the fuel (H_2O, CO_2 or O_2) from thermodynamic point of view [6,7]. The O_2 or O^{2-} can easily oxidize the carbon species into CO and CO_2 under cell operating temperature. Whereas, another strategy is design and modification of anode materials to inhibit carbon formation or remove carbon by water-gas reaction *via* enhanced H_2O adsorption on the anode [8–10]. Furthermore, adding an inter-reforming layer on top of anode which can convert CH_4 into H_2 has also been demonstrated effective at reducing carbon deposition [11].

Semiconductor photocatalysis has been widely studied in degradation of various types of pollutants in aqueous phase and gas phase, since it can *in situ* generate oxidative species including hydroxyl radicals, superoxide radicals *etc.* on surface of photo-catalysts under excitation of proper energetic photons [12–17]. In addition, solid phase mineralization of carbon soot by migrating hydroxyl radicals on TiO_2 powder under UV light irradiation was also reported [18]. In order to utilize the full spectrum of solar light, a series of photocatalysts (*e.g.*, defective oxides) with broad light absorption capacity up to 2500 nm have been developed [19], demonstrating that the photocatalytic redox process can be achieved under longer wavelength (IR range) of solar photons. The heat driven near IR or IR light photoactivity referred as

* Corresponding author at: Institute of Hydrogen and Fuel Cell, Harbin Institute of Technology, Shenzhen, Shenzhen 518055, China.
** Corresponding author.
E-mail addresses: zhangguan@hit.edu.cn (G. Zhang), zoujing@cuhk.edu.cn (J. Zou).

https://doi.org/10.1016/j.cclet.2021.01.050

thermo-photocatalytic activity has been demonstrated at elevated temperature together with a UV–vis lamp for a variety of applications. For example, thermo-photocatalytic CO_2 reduction or hydrogenation on Ru/TiO_2 [20], methane reforming on Pt/black TiO_2 [21], propane oxidation on $Pt/TiO_2/WO_3$ [22], near IR driven water splitting on WO_2-Na_xWO_3 [23] and organic pollutants degradation on $BiO_{2-x}Bi_2O_{2.75}$ [24] *etc.* have been reported recently. Many defective oxides present the thermo-photocatalytic behavior, since the defects on the surface or in the bulk solid oxide semiconductor can yield intermediate energy states between the band−gap and significantly change its optical absorption property and charge carrier mobility. However, highly concentrated defects in an oxide semiconductor can cause the intrinsic change of its conductive property from a semiconductor to a metallic one, and thus the photogenerated charge transition from occupied bands to unoccupied bands cannot be explained by the conventional band-gap theory. For example, a red metallic $Sr_{1-x}NbO_3$ photocatalyst has been demonstrated as an effective photocatalyst for the oxidation of methylene blue and reduction of water, and the authors proposed that the electron transition occurs from the conduction band to a higher level unoccupied band [25]. Recently, we also demonstrated that highly reduced transitional metal oxides (*e.g.*, TiO_{2-x}) can stabilize electrons in the bulk and release them into water upon thermal or near infrared light excitation, corresponding to defects formation upon reduction and removal upon oxidation [26,27], can be repeatedly proceeded.

So far, most of the thermo-photocatalytic processes for liquid/solid phase reaction were carried out under moderately elevated temperature ($T \leq 100\,^{\circ}C$) and gas/solid phase reaction were performed at relatively higher temperature ($T \leq 500\,^{\circ}C$), whereas the thermo-photocatalytic process in a gas/solid/solid triple phase under higher temperature (>500 °C) is still not explored yet. Under condition of such high temperature, intense IR light would be irradiated to a heated solid catalyst, which may induce the charge carriers' transition and then initiate the photocatalytic redox process. Upon this hypothesis, oxidative hydroxyl radicals could be produced on the surface of a semiconducting or metallic solid by oxidizing water or adsorbed hydroxyl group under high temperature.

In this work, we aim to explore the IR-light driven thermo-photocatalytic reactions occurring on a gas/solid/solid triple phase boundary for mineralization of carbon species under high temperature utilizing the *in situ* generated hydroxyl radical as the oxidant, so as to solve the carbon deposition problem on the anode of biogas fueled SOFCs. Firstly, commercial TiO_2 nano-powder was physically mixed into NiO-YSZ based anode, then metallic TiO_x particles can be produced in the composite anode during fabrication of single cell upon the high temperature H_2 reduction process. The introduction of TiO_x particles into anode shows a positive effect on the electrocatalytic activity on the methane oxidation and coking resistance of single cell in simulated biogas fuel. The detailed information on cell fabrication and testing approach were described in supporting information.

From the cross-sectional view of a single cell as shown in Fig. 1a, the optimized single cell was composed by LSM + YSZ/LSM/LSM + LSCF based cathode layer (~100 μm), a dense YSZ electrolyte layer (~50 μm), and TiO_x modified Ni/YSZ anode support layer (ASL, ~700 μm) and TiO_x/Ni/YSZ anode reforming layer (ARL, ~20 μm). In the ARL and ASL, a certain amount of TiO_2 particles were physically mixed with anode powder and converted to TiO_x after H_2 reduction at 850 °C for 5 h, which is expected to play dual roles during cell operation. Firstly, it has been demonstrated that Pt/TiO_{2-x} catalyst can markedly improve the thermo-kinetics of reforming CH_4 to H_2 with a quantum efficiency of 60% at 500 °C under visible light irradiation [21]. More importantly, hydroxyl radical could be generated by thermo-photocatalytic process on

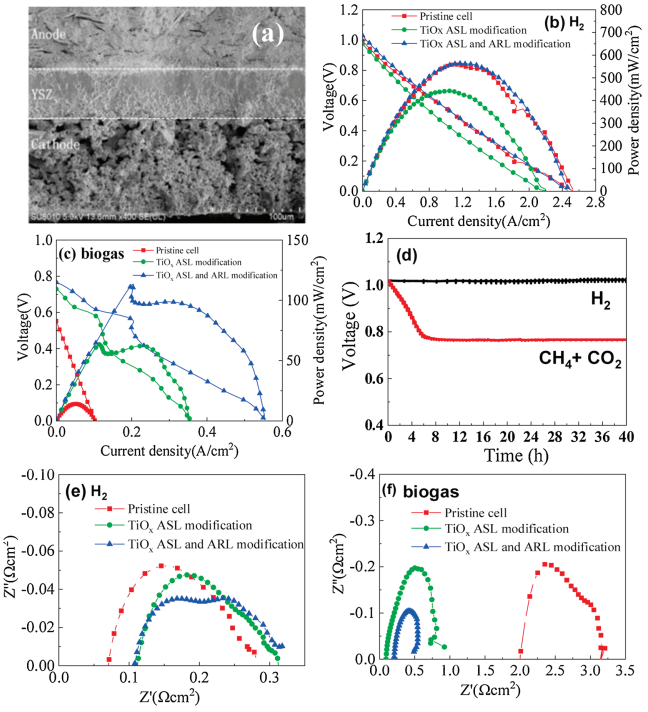

Fig. 1. Structure and performance of original and modified SOFCs. (a) A scanning electron micrograph image of a single cell composed by different layers. *I-V* and *I-P* curves of a single cell operated at 850 °C using (b) H_2 and (c) biogas. (d) Open circuit potential of single cells operated in H_2 or biogas. Impedance analysis of single cells under (e) H_2 and (f) biogas.

TiO_x particles, which can be utilized for deposited carbon oxidation and removal. Through systematic optimization of ratio of doped TiO_2 and ARL components and thickness, we found that the cell composed by 1 wt% TiO_2/Ni-YSZ composite and 3 wt% TiO_2/Ni-YSZ as the ARL exhibited the best electrochemical performance, compared to other cells with different components.

We evaluated the electrochemical performance of the unmodified cell and TiO_x modified cells using H_2 (as reference) and simulated biogas (70% CH_4 + 30% CO_2) mixed with ~ 3% H_2O vapor as the fuel and ambient air was used at 850 °C. Representative *I-V* and *I-P* curves of a single cell are shown in Figs. 1b and c. Under H_2 operating condition, the peak power densities of unmodified cell, 1 wt% TiO_x ASL modified cell and 1 wt% TiO_x ASL and ARL modified cell were 0.559, 0.442, 0.560 W/cm^2 at 850 °C (Tables S1–S4 in Supporting information). The TiO_x ASL modification slightly deteriorated the electrochemical performance, probably because the gas transfer and electrocatalytic activity was inhibited. Whereas the TiO_x ASL and ARL modified cell exhibited similar electrochemical performance with unmodified one. It is commonly considered that the ARL is beneficial for improving electrochemical activity by increasing triple phase boundary length, which can compensate the negative effect introduced by TiO_x introduction. When these cells run in simulated biogas, the peak powder densities of unmodified cell were significantly reduced to ~0.014 W/cm^2 at 850 °C, whereas average peak powder densities of 0.06 and 0.10 W/cm^2 for those of TiO_x ASL modified and TiO_x ASL and ARL modified cells (Tables S1–S4). The distinct differences imply the significant roles of TiO_x and ARL modification. The sharp spike peaks of the power density maybe attributed to the redox reactions during running biogas fuel. The stable open circuit potentials (1.0 V for H_2 and 0.78 V for biogas) for 40 h (Fig. 1d) suggests that the composite anode is robust in direct utilization of methane. The impedance spectra imply that both electrolyte and

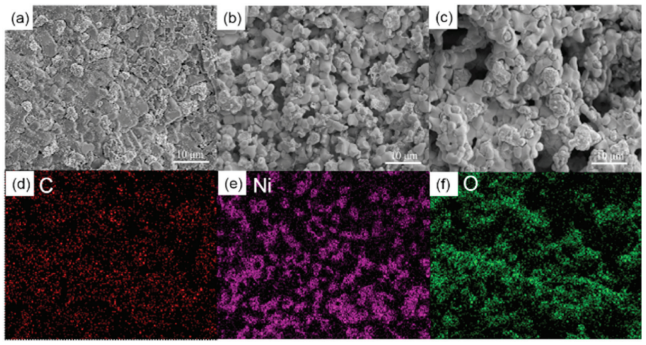

Fig. 2. SEM images of different anodes after reaction: (a) unmodified Ni-YSZ anode. (b) TiO_x modified Ni-YSZ anode. (c) TiO_x ASL and ARL modified anode.EDS images of anode for TiO_x modified anode as shown in panel b: (d) C element; (e) Ni element; (f) O element.

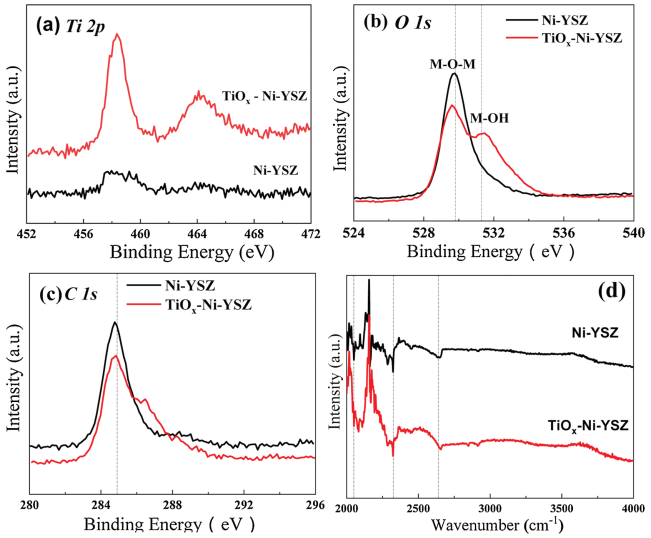

Fig. 3. XPS analysis (a) Ti 2p, (b) O 1s, (c) C 1s and (d) FTIR analysis of Ni-YSZ anode and modified TiO_x-Ni-YSZ anode.

electrodes contribute small ohmic resistances to the total cell resistance under H_2 (Fig. 1e). The ohmic resistance at 850 °C was only about 0.07∼0.10 Ω cm^2 while the polarization resistance was ∼0.20 Ω cm^2, indicating that polarization resistances contribute more to the total cell resistance. When fueled with biogas, the pristine cell exhibited much higher ohmic and polarization resistances which was about 2.0 and 1.2 Ω cm^2 (Fig. 1f), indicating that Ni-YSZ anode has lower catalytic activity for CH_4 oxidation while it has higher activity towards H_2 oxidation. For the TiO_x ASL and TiO_x ASL and ARL modified cells, both of the ohmic and polarization resistances were markedly reduced when fueled by biogas. The results imply that the modified cells have better electrochemical performances towards CH_4 fuel.

In addition, the coking resistance of the composite anode can be clearly presented as shown from the SEM and EDS images of these cells after reaction. For the pristine cell, many carbon particles appeared on the surface of anode after reaction (Fig. 2a and Fig. S1 in Supporting information), whereas the composite cells with TiO_x ASL or TiO_x ASL and ARL modification show less carbon particles deposition on the surface of anode after reaction (Figs. 2b and c). The deposited carbon was further confirmed by EDS mapping images (Figs. 2d–f) showing that O and Ni elements are composed as the backbone components, whereas carbon species homogeneously existed on the anode surface. Some carbon species may come from the sample contamination in the air. Furthermore, the porosity of anode for the unmodified cell after reaction was also reduced due to the carbon deposition, resulting in the decay of its performance.

To gain insights into the enhanced performance of the modified anode, we analyzed the commercial NiO/YSZ powder and 1 wt% TiO_x-Ni/YSZ composite powder, which were pressed and sintered at 1100 °C in air for 2 h and reduced in pure H_2 atmosphere at 850 °C for 5 h. The XRD patterns (Fig. S2 in Supporting information) of the reduced Ni/YSZ and TiO_x-Ni/YSZ composite samples indicate that anatase/rutile phase of TiO_2 at 2θ of 25.7° and 27.6° was disappeared after high temperature reduction, and there are new phases formed at 2θ of 37.2°, 39.6°, 43.3°, 46.7° in the modified anode materials, which can be indexed to titanium oxides (TiO_x) such as TiO (PDF#89-3360), $TiO_{0.975}$ (PDF#75-0312), $TiO_{1.2}$ (PDF#85-1381) and $TiO_{1.69}$ (PDF#89-3076). For further proving the reduction behavior, we carried out the powder reduction experiment under the same reduction condition. White TiO_2 powder can be converted to the nonstoichiometric black TiO_x, which has been reported with reduced band-gap and metallic property [26,27]. XPS analysis of Ni-YSZ anode and TiO_x modified anode clearly shows the difference between the two samples. As shown in Fig. 3a, the weak Ti 2p peaks at binding energies of ∼458 eV and ∼464 eV originate from the doped TiO_x particles in reference with the Ni-YSZ sample. The O 1s peaks are slightly different for the two samples (Fig. 3b), the peak at binding energy of 530 eV can be assigned for M—O—M bonds, whereas the new peak at binding energy of 532 eV for the modified sample can be assigned for M—OH bond. The H_2 reduction creates the oxygen defects and thus the Ti—OH bond may exist at the defect sites. On the other hand, the carbon elements shown for both samples may come from the carbon deposition during cell operation with CH_4 fuel and sample contamination in the air (Fig. 3c). Thus, it is not convincible to quantify the amounts of carbon species on the anode samples by XPS analysis. The FTIR spectra shows little difference between the two samples (Fig. 3d), there was no water absorption peaks appeared at 3450–3550 cm^{-1}. In literature [10], it was found that increasing the absorption of water and surface hydroxyl group on the anode was the key for improving coking resistance performance in direct CH_4 fueled SOFCs with alkaline metal or rare earth metal modified anodes. Therefore, the reduced carbon deposition performance of the TiO_x modified anode should be explained by other reasons.

For demonstrating our hypothesized mechanism accounting for reduced carbon deposition, we carried out the thermo-photocatalytic powder experiments by direct mixing TiO_2 powder with graphite powder together, which was firstly reduced by H_2 and then filled with N_2 and water vapor maintained at 850 °C for 30 h. The mass change of powder and generated gas products were monitored for multicycle tests. As shown in Fig. S3a (Supporting information), the powder mass change was negligible without running the temperature ramping program for the repeated batch 1–3 experiments. However, the total mass of powder was significantly reduced after 30 h reaction at 850 °C for the batch 4–6 experiments in Fig. S3b (Supporting information). The reduced amount of powder with an average value of 27.2 mg far exceed the amount of reduced mass assuming that TiO_2 was completely converted into TiO, indicating that the graphite powder was oxidized to gaseous species (*e.g.*, CO, CO_2, C_xH_y) and removed during the high temperature reaction. The generation of CO_2 was demonstrated from the color change and precipitation occurred in the two gas indexing bottles filled with bromothymol blue and limewater (Fig. S4 in Supporting information), implying that CO_2 was continuously produced during the reaction.

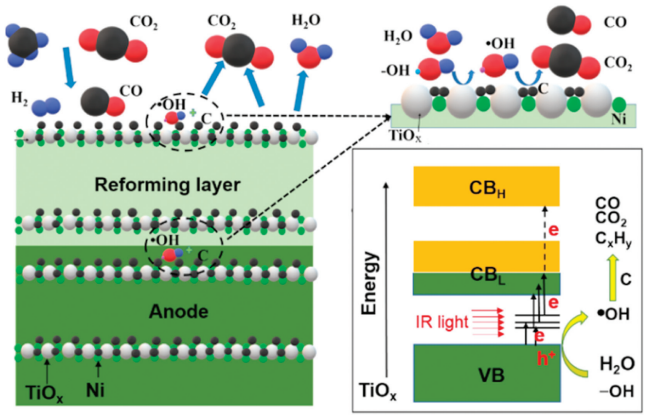

Scheme 1. Proposed mechanism for thermo-photocatalytic removal of carbon deposited on the anode.

The utilization of CH_4 and CO_2 as the SOFCs fuels and the carbon formation process during the high temperature reaction can be expressed by reactions (1) to (5). Furthermore, the addition of reforming layer can partially convert CH_4 into H_2 and improve the cell performance according reaction (6), both the Ni particles and TiO_x particles play the reforming roles at high temperature. The carbon deposition on the anode would cause the decay of electrochemical performance of fuel cells as shown from the unmodified cell. According to the experiments observation, we propose the IR-light driven photocatalytic removal of carbon under high temperature in the direct CH_4 fueled SOFCs through the reactions of (7)–(11).

$$CH_4 + CO_2 \rightarrow 2CO + 2H_2 \quad (1)$$

$$H_2 + O^{2-} \rightarrow H_2O + 2e\text{-} \quad (2)$$

$$CO + O^{2-} \rightarrow CO_2 + 2e\text{-} \quad (3)$$

$$CH_4 \rightarrow C + 2H_2 \quad (4)$$

$$2CO \rightarrow C + CO_2 \quad (5)$$

$$2H_2O + CH_4 \rightarrow 4H_2 + CO_2 \quad (6)$$

$$TiO_2 + H_2 \rightarrow TiO_x + H_2O(850^\circ C) \quad (7)$$

$$TiO_x \xrightarrow{\Delta hv} e^- + h^+(850^\circ C) \quad (8)$$

$$h^+ + H_2O \rightarrow \cdot OH + H^+(850^\circ C) \quad (9)$$

$$h^+ + \text{-}OH \rightarrow \cdot OH(850^\circ C) \quad (10)$$

$$\cdot OH + C \rightarrow CO + CO_2 + C_xH_y(850^\circ C) \quad (11)$$

As shown in Scheme 1, TiO_2 was converted to defective metallic TiO_x, and could be excited by strong IR light irradiation to generate electron-hole pairs by carrier transition from occupied valence band (VB) to lower unoccupied conduction band (CB_L) *via* the mediation of intermediate defects states or from the lower unoccupied conduction band CB_L to a higher unoccupied band (CB_H). The remained holes could oxidation water vapor or surface hydroxyl group to generated oxidative hydroxyl radical, which can be diffused into the vicinity of deposited carbon species and further oxidize them into CO, CO_2 or C_xH_y. The oxidation process took place on the water vapor/carbon/TiO_x triple phase boundary. The generated CO_2 was indirectly demonstrated, however more *in situ* characterization and analysis techniques are required to directly demonstrate the proposed mechanism.

In summary, by integrating TiO_x powder into the Ni-YSZ anode and ARL layer, the SOFCs cell performance was significantly improved when simulated biogas was used as the fuel and ambient air was used as the oxidant. The peak power density was enhanced about seven times for the optimized anodes. More importantly, the coking resistance of the composite anode is exceptional in contrast to the state-of-the-art Ni-YSZ anode. The remarkable performance and stability of the developed fuel cell may result from the IR light driven photocatalytic removal of deposited carbon on the anode, in which *in situ* generated hydroxyl radical is the key oxidant for carbon removal. This work provides a novel strategy for solving the carbon deposition problems in direct methane fueled SOFCs.

Declaration of competing interest

The authors declare that they have no known competing financial interests or personal relationships that could have appeared to influence the work reported in this paper.

Acknowledgments

This work is supported by Shenzhen Science and Technology Innovation Commission (No. JCYJ20190813171403664), Basic research program of Guangdong Province (No. 2018A030313851), Longgang District Technology Supporting Project (No. LGKCKJPT2019074), the Fundamental Research Funds for the Central Universities (No. HIT. NSRIF. 2020074). We also thanks professor Zheng Zhong for providing collaboration research at Institute of Hydrogen and Fuel Cell.

Appendix A. Supplementary data

Supplementary material related to this article can be found, in the online version, at doi:https://doi.org/10.1016/j.cclet.2021.01.050.

References

[1] W. Wang, R. Ran, Z. Shao, J. Power Sources 196 (2011) 90–97.
[2] W. Wang, R. Ran, Z. Shao, Int. Hydrogen Energy 36 (2011) 755–764.
[3] Z. Tao, G. Hou, N. Xu, Q. Zhang, H. Ding, Electrochim. Acta 150 (2014) 55–61.
[4] X. Yao, P. Li, B. Yu, et al., Int. Hydrogen Energy 42 (2017) 22192–22200.
[5] N. Hou, T. Yao, P. Li, et al., ACS Appl. Mater. Interfaces 11 (2019) 6995–7005.
[6] J. Ma, C. Jiang, P.A. Connor, M. Cassidy, J.T.S. Irvine, J. Mater. Chem. A 3 (2015) 19068–19076.
[7] B.J.M. Sarruf, J.E. Hong, R. Steinberger-Wilckens, P.E.V. de Miranda, Int. Hydrogen Energy 43 (2018) 6340–6351.
[8] J. Qu, W. Wang, Y. Chen, X. Deng, Z. Shao, Appl. Energy 164 (2016) 563–571.
[9] D. Yoon, A. Manthiram, Energy Environ. Sci. 7 (2014) 3069–3076.
[10] J. Qu, W. Wang, Y. Chen, et al., ChemSusChem 11 (2018) 3112–3119.
[11] Y. Chen, B. deGlee, Y. Tang, et al., Nat. Energy 3 (2018) 1042–1050.
[12] M. Zhang, J. He, Y. Chen, P.-Y. Liao, M. Zhu, Chin. Chem. Lett. 31 (2020) 2721–2724.
[13] G. Liu, J. Zhou, W. Zhao, Z. Ao, T. An, Chin. Chem. Lett. 31 (2020) 1966–1969.
[14] B. Jing, Z. Ao, W. Zhao, et al., J. Mater. Chem. A 8 (2020) 20363–20372.

[15] H. Xu, J. Shi, S. Lyu, X. Lang, Chin. J. Catal. 41 (2020) 1468–1473.
[16] X. Li, X. Lang, J. Chem. Phys. 152 (2020) 044705.
[17] S. Hu, Y. Yu, Y. Guan, et al., Chin.Chem. Lett. 31 (2020) 2839–2842.
[18] M.C. lee, W. Choi, J. Phys. Chem. B 106 (2002) 11818–11822.
[19] M.Q. Yang, L. Shen, Y. Lu, et al., Angew. Chem. Int. Ed. 58 (2019) 3077–3081.
[20] C. Wang, S. Fang, S. Xie, Y. Zheng, Y.H. Hu, Chemistry 8 (2020) 7390–7394.
[21] B. Han, W. Wei, M. Li, K. Sun, Y.H. Hu, Chem. Commun. 55 (2019) 7816–7819.
[22] L. Wang, X.Y. Liu, A. Wang, et al., Angew. Chem. Int. Ed. 59 (2020) 12909–12916.
[23] G. Cui, W. Wang, M. Ma, et al., Nano Lett. 15 (2015) 7199–7203.
[24] M. Wang, G. Tan, D. Zhang, et al., Appl. Catal. B: Environ. 254 (2019) 98–112.
[25] X. Xu, C. Randorn, P. Efstathiou, J.T.S. Irvine, Nature Mater. 11 (2012) 595–598.
[26] X. Zhang, G. Zhang, J. Zou, New J. Chem. 42 (2018) 6084–6090.
[27] G. Zhang, J. Zou, X. Xu, Adv. Sustain. Systems 2 (2018) 1700139.